JOURNAL OF MATERIALS SCIENCE 20 (1985) 1093–1104

Thermophysical properties of asbestos-reinforced rubbers

P. LOFTUS*, J. O'DONNELL†, G. H. WOSTENHOLM, B. YATES
Department of Pure and Applied Physics, University of Salford, UK

D. V. BADAMI‡, D. GREEN
TBA Industrial Products Ltd, Rochdale, UK

Factors influencing the sealing characteristics of gaskets made from asbestos-reinforced rubbers include mechanical properties, thermal properties and moisture absorption characteristics. Existing knowledge of the temperature dependence of the mechanical behaviour has been augmented by investigations of the specific heat capacity, thermal expansion and thermal conductivity at temperatures up to 250° C, as well as moisture absorption characteristics at ambient temperature of as-prepared and thermally cycled material. The measurements have provided an insight into thermally induced structural changes within the matrix, which are relevant to component operation.

1. Introduction

Among the properties of chrysotile asbestos that give it an important place in the range of fibres available to composite manufacturers are its abilities to resist heat, moisture and corrosion. Coupled with its high tensile strength and flexibility, its minimal tendency to acquire an electric charge and its fibrous structure, it is ideally suited to applications in textiles and in composites where good dispersion of the reinforcement inclusions within the matrix is required.

The application in connection with which the present investigation arose was that of composite gaskets for cylinder heads in internal combustion engines. These consist typically of 70% asbestos fibre dispersed within a matrix of rubber and operate over the temperature range 20° C to 350–400° C. Factors influencing the performance of a gasket material are its elasticity, moisture absorption characteristics and thermal expansion behaviour. Other physical properties having immediate technological significance in the present application, which also provide fundamental scientific information concerning the behaviour of the material on an atomic/molecular scale, are the specific heat capacity and thermal conductivity. Partly to elucidate a peculiarity observed in the temperature dependence of the elastic behaviour and partly in order to provide information of value in a wider context, a survey of selected physical properties of representative gasket materials has been undertaken. This supplements thermal data for related materials obtained in these laboratories a few years ago [1].

2. The gasket composite and its constituent materials

2.1. Chrysotile asbestos

The structure of chrysotile asbestos has been described elsewhere (e.g. [2]). It is unaffected by heat up to 450 to 500° C, which is considerably higher than the highest temperature reached during the present series of experiments, i.e. approximately 250° C. Its particular attractions for application in gaskets have already been described and it has been so employed in the automobile service industry for many years.

2.2. The matrix material

In order to understand the temperature

*Present address: Electronics and Measurement Techniques Department, Rolls-Royce Ltd, Derby, UK.
†Present address: Department of Science and Humanities, Darlington College of Technology, UK.
‡Present address: T and N Materials Research Ltd, Rochdale, UK.

0022–2461/85 $03.00 + .12

dependence of some of the physical characteristics of the composite materials it will be instructive to consider the principal structural features of the rubbers in the matrix and details of the curing process employed during manufacture. The matrices commonly employed in gaskets consist of a mixture of natural rubber with a synthetic rubber. One such synthetic rubber is styrene butadiene rubber (SBR), which is produced by the polymerization of butadiene and styrene to form long copolymer chains. The addition of SBR to natural rubber improves the resistance to abrasion and weathering. Another synthetic rubber employed in gaskets is nitrile butadiene rubber (NBR), the addition of which to natural rubber improves the resistance to petroleum oils.

The object of vulcanization is to link the long polymer chains together, producing increased strength while preserving some of the elasticity [3]. Sulphur is commonly employed in curing natural rubber and SBR, in which it dissolves in the form of eight-membered rings, but it dissolves less rapidly in NBR. The process of vulcanization consists of breaking these rings with the aid of organic accelerators and metallic oxides at elevated temperatures, following which the resulting sulphur chains form links between the polymer molecules. It will be seen later that carbon cross-links were employed in the formation of an elastomer during a later stage of the investigation. This was achieved with the aid of dicumyl peroxide, which was activated by heating. The activation is transferred to the polymer chain by the removal of a hydrogen ion from a CH_2 group, leading to the formation of a carbon–carbon bond between a pair of such groups in neighbouring polymer chains.

The tensile strength of rubber increases as the density of crosslinks increases, reaching a maximum at approximately 3% sulphur content [3]. At higher levels of sulphur, irregular crosslinking tends to occur. This leads to the network becoming overstrained, individual crosslinks break and the tensile strength falls. At still higher levels of sulphur the tensile strength increases again as the crosslinking becomes more regular.

2.3. The composite

The gasket material is commonly known as CAF* (compressed asbestos fibre). Although not an accurate description of its composition, which includes rubber, the term has found favour in the industry and will be used throughout the rest of this account.

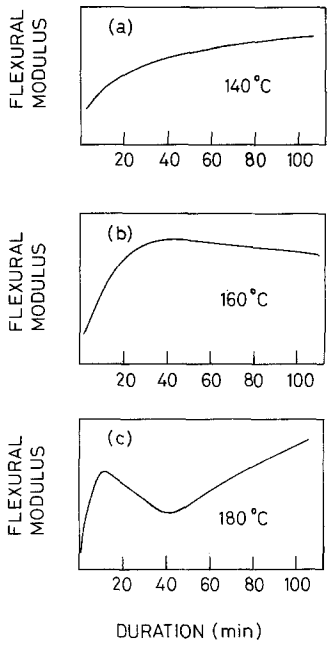

Figure 1 The influence of temperature upon the dependence of the flexural modulus (measured in arbitrary units) of CAF upon time into the vulcanization period.

The progress of the cure of any particular mix of CAF is monitored by checking the flexural modulus of one small sample taken from the bulk, as a function of time at a constant temperature. The results of three such checks are shown in Fig. 1. Reference to results such as those depicted in Fig. 1a shows that up to a temperature of approximately 150° C the modulus increase steadily, finally attaining a maximum value at which it levels off. This behaviour is presumably consistent with a steady increase in the density of crosslinks up to some maximum value. Samples monitored at 150 to 160° C display this behaviour in the early stages of cure but eventually their modulus falls off, as illustrated in Fig. 1b. Reference to Fig. 1c shows that at higher temperatures still the behaviour is even more complicated, the rise and fall being followed by a further rise to a higher modulus. However, the reason for behaviour such as that depicted in Figs. 1b and c was not known at the outset to the present work, as CAF contains less than 3% sulphur, and this was the reason for embarking upon an investigation of the temperature dependence of its specific heat

*CAF is a registered trademark of TBA Industrial Products Ltd.

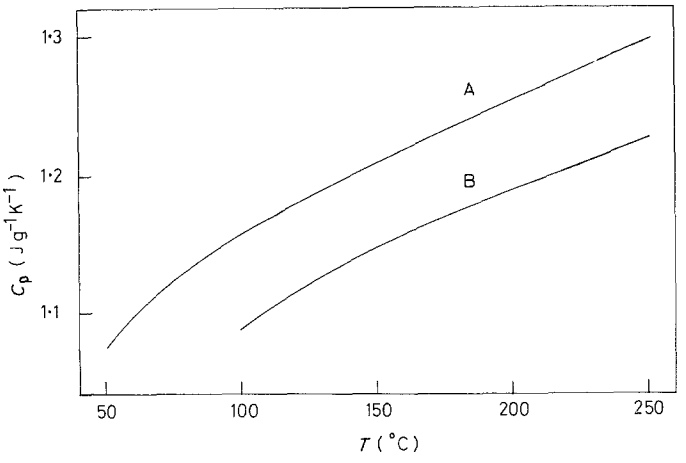

Figure 2 The specific heat capacity, C_p, of Serpentine rock: A, present work (sample from Quebec Province, Canada); B, Leonidov [6] (sample from Kraka Massif, Southern Urals).

capacity. As already indicated, measurements were later extended to other physical properties of this material.

3. Specific heat capacity

3.1. The apparatus and its performance

The apparatus employed for the present work was that described by Casey and Yates [4]. Before being modified to a more convenient form for the purposes of the present investigation, the apparatus was first checked by measuring the specific heat capacity of high-purity single-crystal sapphire over the approximate temperature range 20 to 300° C. The results of these measurements agreed with the NBS results of Ditmars and Douglas [5] within the combined experimental uncertainties over the entire temperature range.

3.2. Chrysotile asbestos

In order to ascertain whether of not the fibrous reinforcement was displaying any abnormalities in its thermophysical behaviour at elevated temperatures, the apparatus was next employed, in its original form, to investigate the specific heat capacity of chrysotile asbestos. The precision of the measurements improves with the ratio of the mass of the specimen to the mass of the calorimeter. It proved to be difficult to achieve a density higher than approximately 1500 kg m^{-3}, by compressing the fibre and so Serpentine rock was employed for this part of the investigation. Serpentine rock bears chrysotile fibre, with which it shares the same chemical composition, but it has a density of approximately 2500 kg m^{-3}, which is the theoretical maximum for the compressed fibre. The results of the measurements upon this sample of rock, which came from the Quebec Province of Canada, are compared with the results of Leonidov [6] for a sample of Serpentine rock taken from the Kraka Massif, Southern Urals, in Fig. 2, The absolute difference between the results, approximately 5%, may be a result of different chemical purities. The important point to notice in the present context is the absence of any unusual behaviour in the specific heat capacity, which might have been associated with the influence of temperature upon the dependence of the flexural modulus of CAF upon time measured into the vulcanization period, illustrated in Fig. 1.

3.3. The composite

3.3.1. Measurement details

Attention was then directed towards the matrix and because this was most readily available in association with the asbestos reinforcement, the specific heat capacity of CAF was investigated next.

Experience gained during the proving work indicated that improved temperature control of the various components of the apparatus might be achieved by controlling the temperatures of the two shields surrounding the calorimeter separately. Appropriate modifications were, therefore, made to the apparatus before proceeding. Estimates indicated that the precision attainable with the apparatus could be improved upon significantly by dispensing with the calorimeter altogether in the work involving CAF. The procedure adopted in this part of the investigation was therefore to fabricate two cylindrical specimens of different mass, each bearing adjuncts (i.e. heaters, thermocouples, etc.) of identical thermal capacity. The specific heat capacity of CAF could then be

TABLE I The composite systems*

	Mix 1		Mix 2		Mix 3
	(a)	(b)	(a)	(b)	
Matrix†	NR/SBR	NR/SBR	NBR	NBR	NR/NBR
Curing system	Sulphur + accelerators	Dicumyl peroxide	Sulphur + accelerators	Dicumyl peroxide	Sulphur + accelerators
Fibre	Chrysotile	Chrysotile	Chrysotile	Chrysotile	Chrysotile
Fillers	Barytes	Barytes	Barytes	Barytes	Barytes
Solvent	Toluene	Toluene	Toluene	Toluene	Toluene

*These are "model" systems which are not typical of commerical products.
†NR, natural rubber; NBR, nitrile butadiene rubber; SBR, styrene butadiene rubber.

calculated by subtracting the thermal capacity of one assembly from that of the other. The specimens for the various measurements were prepared from the constitutents listing in Table I. These were mixed together until an even distribution of fibre had been achieved, following which the putty-like resultant material was dried at ambient temperature. The dry material was subsequently compressed in a mould to produce solid cylinders of diameter 43 mm and length 46 mm. After being drilled to accommodate the heater and thermocouple, additional holes were drilled in one of the specimens in order to reduce its mass below that of the other specimen.

3.3.2. Results

Because the matrix cures as it is heated, it was necessary to ensure that the same heating rate was employed when investigating both members of a pair of specimens. Each member of the pair of specimens I (see Table II) was recycled over the approximate temperature range 30 to 200° C three times. The results of the measurements made during the course of these excursions are compared in Fig. 3. One may observe a distinct difference between the results of runs 1 and 2, whereas the results of runs 2 and 3 agreed with one another within the limits of experimental uncertainty.

It will be seen later that uncertainties surrounding interpretation of these results led to a wish to investigate the specific heat capacity of a system in which a different curing agent was employed. The results of measurements conducted upon specimens prepared from these samples are compared with those just considered in Fig. 4.

3.3.3. Discussion

3.3.3.1. Sulphur-cured specimens. The two cylinders which together constitute specimens 1 were compressed in a mould during fabrication, as described above. In order to simulate the thermal history of commercially calendered material the cylinders were held in the mould at a temperature of 100° C for 15 min. This was to allow at least 80% of the sulphur to form crosslinks of eight atoms length between carbon atoms in adjacent chains, as illustrated in Structure I.

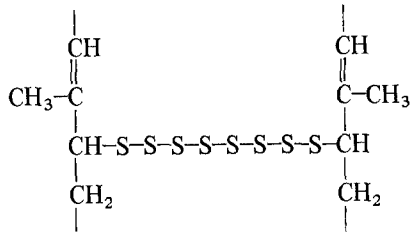

(I)

The variation in flexural modulus must be due to a further change in the crosslinked CAF. The changes in specific heat capacity on the first runs (Fig. 3) clearly relate to this. Between B and C in Fig. 3 one may associate the rise of specific heat capacity with the absorption of energy by the S–S bonds within the crosslinks. This results in the breaking of the crosslinks producing shorter sulphur chains. This gives rise to a corresponding reduction in the flexural modulus as indicated in

TABLE II The specimens

	Mix 1a	Mix 1b	Mix 2a	Mix 2b	Mix 3
Specific heat capacity	1	2	–	–	–
Thermal expansion	3	–	–	–	4
Thermal conductivity	5	6	–	–	–
Moisture absorption	–	–	7	8	–

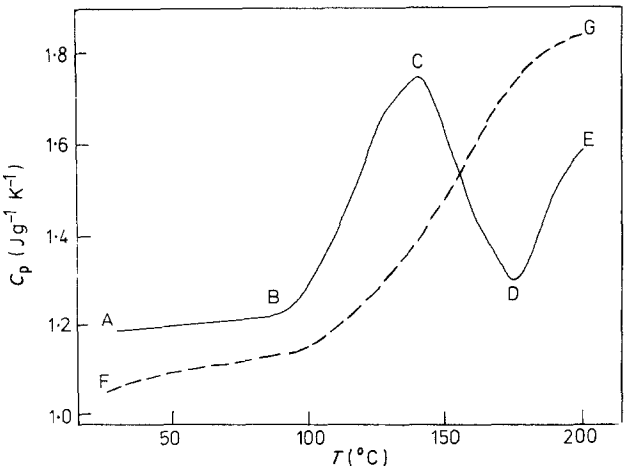

Figure 3 The specific heat capacity, C_p, of specimens 1: —— run 1, – – – runs 2 and 3.

Fig. 1b. Between C and D, with the aid of the accelerators in the material mix, the short chains attack the double carbon bonds in the polymer chain and form new shorter crosslinks. This gives rise to an increase in the flexural modulus to an even higher value than originally observed (Fig. 1c). This occurs because the crosslink density has increased. The energy absorption between D and E may indicate a further alteration in the length of the crosslinks. This interpretation is further borne out by the thermal expansion measurements, as discussed in Section 4.3, where it is indicated that the crosslinks may consist of two sulphur atoms. A representative section of the modified crosslink pattern might look as shown in Structure II.

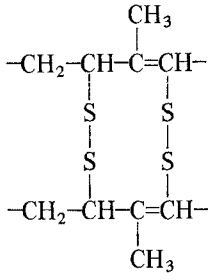

(II)

The fact that F is lower than A in Fig. 3 may be associated with the structural changes which occurred during the first run. The fact that there is no peak in FG corresponding to the peak BCD in AE supports the association of the unique features of AE with bond re-arrangement such as those proposed. The fact that G is above E indicates that further curing occurred after cooling down from the end of the first run. The fact that the results of runs 2 and 3 are coincident indicates that curing was complete at the beginning of the second run. This being so, one might conclude that a slower rate of temperature in run 1 would have produced a value of E at G. Generalizing from this observation, one should note that the exact shape of curve AE must have been governed by the (common) rate at which the temperature was raised during the course of the first run on each of the pair of specimens involved. Also, in a large assembly of atoms and molecules one should realistically expect more than one physical process to be going on at any one time. Taking these two points together, the interpretations proposed have the status of indications of processes which might reasonably be expected to predominate in the different temperature regions examined, following the thermal treatment experienced by these particular specimens.

3.3.3.2. Dicumyl peroxide-cured specimens. In an attempt to obtain supporting evidence for the foregoing interpretation of observations in terms

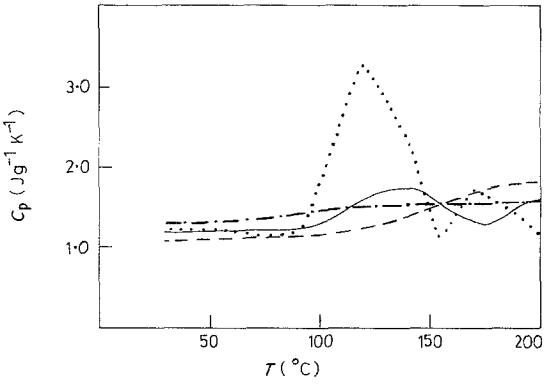

Figure 4 The specific heat capacities, C_p, of specimens 1 and 2: —— 1st run with specimens 1; – – – – subsequent run with specimens 1; ..... 1st run with specimens 2; –·–·– subsequent run with specimens 2.

of bond formation and re-arrangement, mix 1b (Table I) was made up employing dicumyl peroxide as the curing agent, in place of sulphur. The final product in this case is believed to have contained crosslinks between carbon atoms in adjacent chains as shown in Structure III. The specific heat capacity of a pair of specimens was measured as before and the results are compared with the results for the sulphur-cured specimens in Fig. 4.

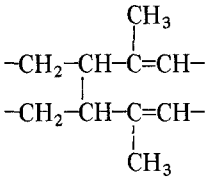

(III)

The mechanism by which the linking of adjacent chains is induced in the case of specimens 2 is believed to be a three stage process. First the dicumyl peroxide molecule is believed to break up into two smaller molecules upon being heated, each of which has a free radical. During oxidation, the free radical is effectively transferred to a polymer molecule, pairs of which then crosslink in the manner illustrated above. The fabrication of these specimens employed cold pressing and it is, therefore, reasonable to associate at least part of the large peak in the specific heat capacity results with the activation of the dicumyl perioxide, which is known to be a relatively slow process occurring within the temperature range in question, i.e. approximately 90 to 150° C. The remaining structural re-arrangements would involve the transfer of energy and the large peak is probably the resultant of the various separate changes involved. The second peak is probably to be associated with driving off the compound shown in Structure IV, which is formed during the transfer of the radical to the polymer chain.

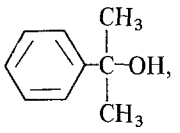

(IV)

Results obtained during a representative subsequent temperature excursion share the absence of anomalies in the results obtained during the second and third runs with specimens 1. This similarity in the contrast of the forms of successive runs of specimens cured in different ways adds credence to explanations based upon molecular structural re-arrangements such as those proposed. Additional evidence is provided by the consistency of the explanations with observed mechanical properties of chemically similar specimens produced according to related temperature cycles. The absolute difference between the results for the fully cured specimens presumably reflects vibrational differences resulting from their different structures.

4. Thermal expansion

4.1. The apparatus and its performance

Specimens for thermal expansion measurements took the form of rods having square cross-sections, length approximately 50 mm and side approximately 7 mm. These rested on the base of a quartz tube, to the top of which was clamped a mechanically operating dial gauge reading to 2×10^{-3} mm. Any length change of the specimen was communicated to the gauge by a second quartz tube, which made contact with the probe of the dial gauge at the top and with the top of the specimen at the lower end. The lowest 80 mm of the quartz tube projected through a hole, plugged with woven asbestos cord, into an oven. The temperature of the oven was raised in increments of approximately 10° C at a rate of approximately 40 to 45° C h^{-1}, between steady values of which readings were taken. This heating rate corresponds closely to that employed in the specific heat capacity work. The temperature of the specimen was measured with a chromel/alumel thermocouple implanted within it, the tip being protected by thermal cement. Because of the self-compensating nature of the design, corrections were necessary only for the outer quartz tube corresponding to the length of the specimen, i.e. approximately 50 mm. The dial gauge itself was some 500 mm above the oven and no corrections to its readings were necessary.

The apparatus was first checked by measuring the linear thermal expansion coefficient of copper between 20 and 250° C. These results agreed with the NBS results of Hahn [7] over the entire temperature range, within the limits of the combined experimental uncertainties.

4.2. Results

The dimensional response to change of temperature may be expressed alternatively as expansivity, $\Delta L/L$, or linear thermal expansion coefficient, α, $[= (1/L)(dL/dT)]$. Employing the former

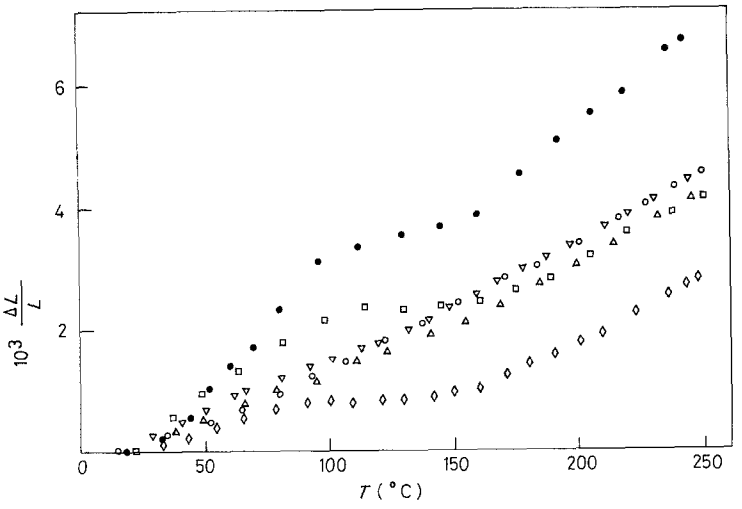

Figure 5 The thermal expansivity, $\Delta L/L$, of specimen 3: • run 1; ○ run 2; □ run 3; △ run 4; ▽ run 5; ◇ run 6.

representation to bring out the differences between the accumulated length changes produced by successive sweeps of the same temperature range, Figs. 5 and 6 illustrate a clear reduction of such integrated dimensional changes for specimens 3 and 4 (see Tables I and II). Detailed examinations of the time/temperature history of the specimens during these excursions, coupled with observations of condensation within the outer quartz tube, have led to the conclusion that much of the reduction of $\Delta L/L$ during successive cycling might be attributed to moisture being driven out of the specimens during heating and absorbed between successive runs.

One striking feature of the results is the similarity of the behaviour of the specimens of the two materials. This similarity is brought out in Fig. 7, in which the linear thermal expansion coefficients of the two specimens are compared with one another. The relatively large scatter in the early results in the first runs on both specimens may be attributed to the relaxation of residual stresses, while the essential similarity between the two sets of results indicates that the different monomers used in each specimen, styrene and acrylonitrile, do not affect either the curing mechanism or the process of moisture absorption.

Fig. 7 is also used to make a qualitative comparison of the temperature dependences of the thermal expansion with the specific heat capacity results for the SBR specimens during their first runs. The samples were hot pressed, ensuring that at least 80% of the material was in the initial state of cure, having crosslinks consisting of eight sulphur atoms.

4.3. Discussion

Initially both the specific heat capacity, C_p, and linear thermal expansion coefficient, α, remain essentially constant. It appears that as the

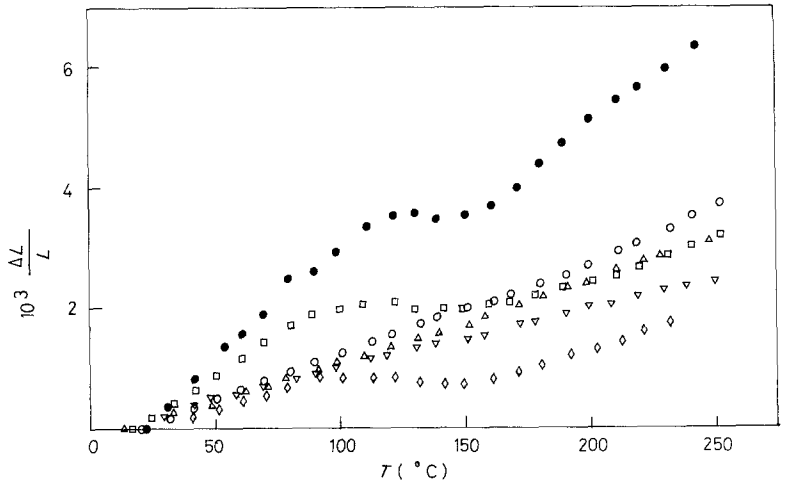

Figure 6 The thermal expansivity, $\Delta L/L$, of specimen 4: • run 1; ○ run 2; □ run 3; △ run 4; ▽ run 5; ◇ run 6.

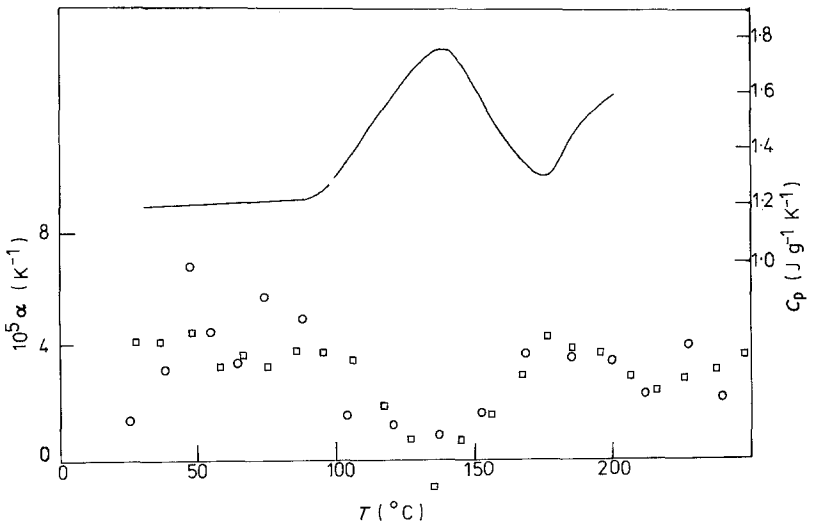

Figure 7 Comparison of the temperature dependence of the specific heat capacity, C_p, of specimens 1 (——) with the linear thermal expansion coefficients, α, of specimens 3 (○) and 4 (□).

temperature increases beyond 100° C the sulphur crosslinks break. The breaking of the crosslinks may then increase the number of transverse modes of vibration available to the polymer chains with a consequent increase in C_p and decrease in α. As the temperature continues to increase, the sulphur may be expected to attack the double bonds in the polymer chains forming crosslinks of length less than eight atoms. C_p now falls and α increases as the new crosslinks restrict the number of transverse vibrations available. The second dip in α suggests that there is a further breaking and reforming of the crosslinks of two atoms length. The intermediate state mentioned above may contain crosslinks of three to six sulphur atoms in length.

It is worth emphasizing that the above changes will not occur in a strict sequence as the temperature increases. As the long sulphur crosslinks break, some of the sulphur will immediately start to form shorter crosslinks. The variations found in both C_p and α indicate which change is dominant as the temperature increases. As already mentioned, the heating rate was arranged to be essentially the same for both the specific heat capacity and the thermal expansion specimens, thus facilitating a meaningful comparison of the temperature dependences of the two quantities.

It was explained earlier that the flexural modulus fell and rose again for curing temperatures of approximately 140° C upwards. This also agrees well with the above interpretation, which is consistent with the smaller crosslink formation taking place between 140 and 180° C.

5. Thermal conductivity

5.1. Experimental arrangements

The thermal conductivity of CAF was measured using commercially produced apparatus, namely model TCFCM N 20-R produced by the Dynatech Corporation. Briefly, the specimen is sandwiched between two identical specimens of a reference material of known thermal conductivity. These are held between a heater and a liquid-cooled heat sink and heat flow through the stack establishes a temperature gradient across it. In order to minimize unwanted heat exchanges the stack was surrounded by a guard, along which a temperature gradient was maintained which was identical to that along the stack itself. The temperature difference across the test specimen and the two reference specimens were measured with chromel/alumel thermocouples situated near the surfaces. At equilibrium, assuming that the heat flow across the stack was uniform and constant, the unknown thermal conductivity could be calculated. An auxiliary heater between the lower reference specimen and the heat sink permitted the stack to be stabilized at a series of different temperatures.

The thermal conductivities of specimens 5 (sulphur-cured) and 6 (dicumyl perioxide cured), described in Tables I and II, were measured as functions of temperature employing this apparatus. The specimens were fabricated by pressing together eight layers of sheet CAF cut to size, which allowed the thermocouples to be located in the body of the material. Each block measured 63.5 mm square by 19.0 mm deep. The thermocouples were situated between the first and

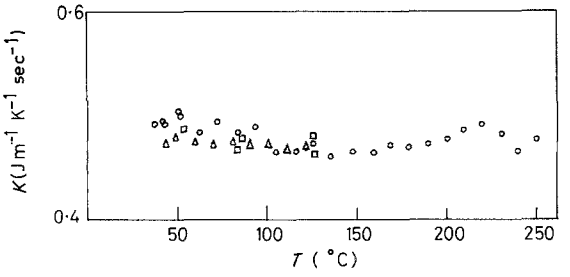

Figure 8 The thermal conductivity, K, of specimen 5: ○ run 1; □ run 2; △ run 3.

second layers, and the seventh and eighth layers, respectively.

5.2. Results

The results of the measurements on specimen 5 are shown in Fig. 8. After confirming the reproducibility of the results through runs 1 and 2, a third run was executed some three months later in order to test for a time dependence which might have been associated with effects such as moisture absorption, chemical changes, etc. As the figure shows, no such time dependence was observed. The results for specimen 6 are shown separately in Fig. 9, for clarity, although they are essentially identical to the results for specimen 5, indicating that the thermal conductivity was not significantly influenced by the change in composition of the curing agent.

5.3. Discussion

Apart from the identity of their magnitudes, the most striking feature of the results for specimens 5 and 6 is their independence of temperature. In fact the values are centred around $0.45 \pm 0.05\,J\,m^{-1}K^{-1}sec^{-1}$ over the entire temperature range covered in the investigations, i.e. 40 to 250° C. The greater part of the error limits arose from uncertainty in the exact separation of the thermocouples.

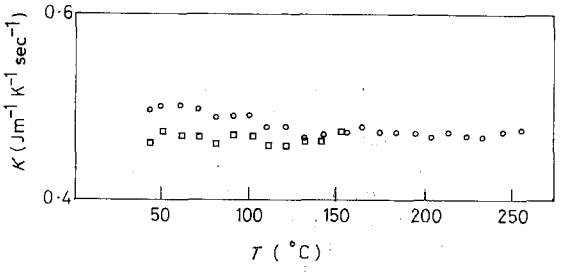

Figure 9 The thermal conductivity, K, of specimen 6: ○ run 1; □ run 2.

The insensitivity to change of temperature is reminiscent of the behaviour of imperfect crystals and structurally disordered glasses. In such systems transverse waves are rapidly attenuated, the mean free path is essentially constant with a value of the order of the interatomic distance and the thermal conductivity follows the temperature dependence of the specific heat capacity. There is an analogy with CAF, which contains many inter-phase boundaries and voids which may be expected to dominate the scattering process, leaving effects due to differences of curing history and moisture content negligible in comparison. The recognition of an unambiguous correspondence of behaviour of the specific heat capacity and thermal conductivity would require an extension of the measurements to lower temperatures. Such an extension lay outside the terms of the present investigation but the evidence we do have is broadly consistent with an explanation in the above terms.

6. Moisture absorption characteristics

6.1. Background

The presence of moisture in a sealing gasket significantly affects two of its important properties, the gas leakage and the tensile strength.

During the course of routine quality control tests it has been established that the sealing characteristics of CAF gaskets improves markedly as the moisture content rises to 2 or 3%. Unfortunately, the tensile strength of the material decreases with increase in moisture content and experience shows that 1% is the acceptable upper limit for the majority of practical applications. Clearly the moisture absorption characteristics of the material are very important to its usefulness. For this technological reason the present investigations were extended to cover studies of moisture absorption in as-produced samples of CAF, cured using sulphur and dicumyl peroxide, and sulphur-cured material which had been heat cycled.

6.2. Experimental details

All the samples were prepared by the standard production process to produce flat sheets. In the course of the process the material experienced only sufficient heating to remove the process volatiles. For sulphur-based systems, this gave a material in which all the sulphur had been activated with the greater part of it having formed sulphur crosslinks. For dicumyl peroxide systems,

where the activation of the peroxide is slower, the equivalent degree of crosslinking was believed to be substantially lower. Two sets of samples were examined, covering both curing systems. The moisture absorption characteristics were monitored for as-calendered material and in the case of the sulphur cured system for material which had been heated to 250° C in air.

The basic material for all samples was the same, except for the curing components, and consisted of an NBR matrix with chrysotile fibre (Tables I and II). Each calendered sheet, nominally 2 mm thick, was cut into rectangular specimens, nominally 50 mm x 25 mm. The orientation of the specimens with respect to the production of the sheet from which they were cut was always the same. The significance of any difference between absorption characteristics through the long and short faces, therefore, was to be associated with preferential fibre orientation occurring during the production process. The specimens were coated with Apiezon vacuum wax on four sides, thus producing specimens with the two faces open, the two long sides open or the two short sides open. The specimens were weighed dry (having been stored in a desiccator containing silica gel crystals between being produced and coated), before and after being waxed. They were then transferred to trays within a series of desiccators, in the bottoms of which saturated solutions of various salts were employed to create atmospheres with a range of humidities. By weighing the specimens periodically the moisture absorption in different directions was monitored as a function of time for five or six levels of humidity between approximately 20% and 100%. It was established in a subsidiary experiment that absorption by the wax was negligible in comparison with absorption by the CAF. Measurements indicated that the room temperature did not fluctuate by more than ± 3° C during the course of the observations and salts were chosen such that the humidities above saturated solutions of them did not display a variation in humidity over this temperature range.

6.3. Results

In an attempt to safeguard against material variability, specimens were generally employed in batches of four, from observations upon which averaged results were evaluated. An exception was provided by the sulphur-cured (as-calendered) specimens for which only single examples of specimen 7 were available. Fig. 10 illustrates a family of curves containing the averaged results for each of three typical batches of specimens conditioned at one level of humidity. A common feature of most such families of graphs is their failure to level out at exactly the same equilibrium moisture content. Since each batch of specimens was subjected to identical conditions one is driven to conclude that this must be a reflection of material variability, e.g. a variation in surface microcrack density. This implies that batches of four specimens were not as large as one might have employed to obtain more representative averages for this system. However, these variations in equilibrium moisture content were not serious and the diffusivity was calculated from the graphs by employing the process of successive approximation described by Shen and Springer [8]. The results of these calculations are summarized in Table III.

6.4. Discussion

A study of the results contained in Table III leads

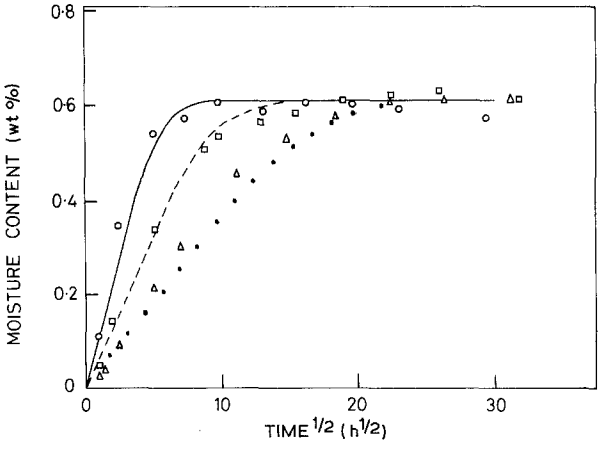

Figure 10 A typical family of curves, illustrating different averaged rates of moisture absorption by the various faces of a batch of four specimens measuring 50 mm × 25 mm. These results refer to dicumyl peroxide cured CAF in the as-calendered condition, exposed to a relative humidity of 65%. Faces open: ○ experiment; —— calculated. Long sides open: □ experiment; – – – calculated. Short sides open: △ experiment; . . . calculated.

TABLE III Diffusivities and equilibrium moisture levels

Relative humidity (%)	Faces open		Long sides open		Short sides open		Average equilibrium moisture level (wt %)
	Diffusivity ($mm^2\ h^{-1}$)	Equilibrium moisture level (wt %)	Diffusivity ($mm^2\ h^{-1}$)	Equilibrium moisture level (wt %)	Diffusivity ($mm^2\ h^{-1}$)	Equilibrium moisture level (wt %)	
Sulphur cured CAF (as-calendered)							
22	0.025	0.13	1.61	0.13	1.01	0.13	0.13
33	0.023	0.26	0.94	0.26	1.00	0.27	0.26
43.5	0.020	0.39	1.16	0.44	1.29	0.42	0.42
65	0.015	0.80	1.06	0.81	0.98	0.79	0.80
97	0.005	5.25	0.13	6.25	0.21	6.25	5.92
Sulphur cured CAF (heat treated)							
22	–	–	1.12	0.21	1.64	0.23	0.22
33	0.017	0.36	1.00	0.35	1.53	0.40	0.37
43.5	0.017	0.47	1.02	0.47	1.42	0.51	0.48
65	0.016	0.87	1.15	0.92	1.39	0.87	0.89
81	0.010	1.76	0.60	1.74	1.24	1.43	1.64
97	0.003	6.70	0.14	6.70	0.27	5.50	6.30
Dicumyl peroxide cured CAF (as-calendered)							
33	0.026	0.21	1.21	0.22	1.59	0.21	0.21
43.5	0.032	0.33	1.23	0.33	1.79	0.32	0.33
65	0.027	0.61	1.52	0.61	1.73	0.62	0.61
81	0.021	1.38	0.75	1.39	1.02	1.41	1.39
97	0.003	8.20	0.12	8.40	0.25	8.20	8.30

to the following general conclusions concerning the diffusivity:

1. the diffusivity is essentially independent of the relative humidity;

2. there is no consistent evidence for the influence of direction upon diffusivity for in-plane absorption;

3. diffusivity through the edges is much higher than it is through the faces. This can be explained by the nature of the calendering process, which gives rise to rubber-rich outer layers (the two faces of a sample). The edges are much more fibrous;

4. the diffusivity of sulphur cured CAF is not significantly influenced by heat treatment;

5. the diffusivity of as-calendered specimens of CAF is not significantly affected by a change of curing agent from sulphur to dicumyl peroxide.

Fig. 11 shows plots of equilibrium moisture content, M_m, against relative humidity, H, from which it is clear that these are related by an equation of the form

$$M_m = aH^b$$

where a and b are constants.

Results corresponding to absorption at a relative humidity of 97% do not fit into these patterns of behaviour. One possibility for this non-conformity may be that the combined effects of a high relative humidity and microcracks is to favour higher absorption than occurs at lower humidity levels. Another possibility is that the high concentration of water molecules favours a degree of chemical bonding to polar sites in the rubber and the asbestos, in addition to physical diffusion. In this case the absorption would not be expected to be Fickian.

7. Summary

It has been explained that at the outset to this investigation it was known that the sealing properties of gaskets fabricated from asbestos-reinforced rubbers were improved by the absorption of a small quantity of water. It was also known that too much water had an adverse effect upon the mechanical properties and it had been observed that the flexural modulus exhibited a time-dependent variation during the vulcanization process, the form of which depended upon temperature.

These observations led to three separate investigations of thermal properties of the material. The temperature dependences of these properties are consistent with an explanation which takes account of the breaking and re-arrangement of bonds between polymer chains during the course of the vulcanization process. The details of these

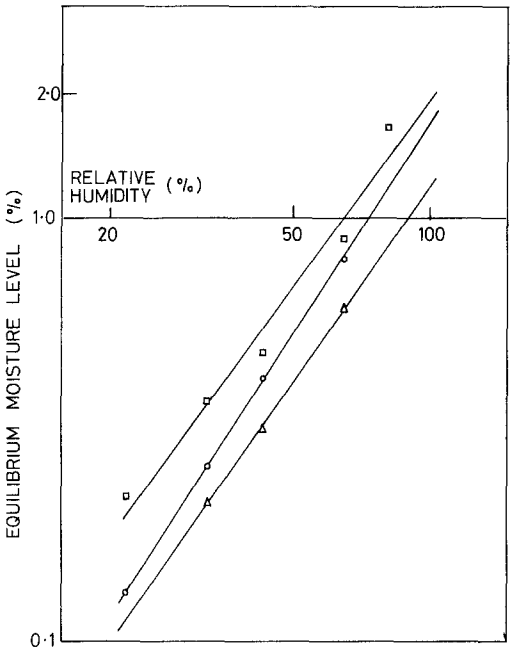

Figure 11 Graphs illustrating the dependence of equilibrium moisture level upon relative humidity: ○ sulphur-cured CAF (as-calendered); □ sulphur-cured CAF (heat treated); △ dicumyl peroxide cured CAF (as-calendered).

structural changes are closely related to details of thermal history, but at least some of the properties of the final product were not found to be critically dependent upon the identity of the curing agent. In addition to leading to a better understanding of the physical processes accompanying cure, the thermal data have technological interest in their own right. Because of their direct relevance to the application of CAF in gaskets, the investigations were extended to include the acquisition of moisture absorption data for a series of representative specimens. The observations suggest that these properties are not critically dependent upon curing agent or heat treatment.

Clearly there is scope for more extensive investigations which would allow the threads to be pulled closer together, e.g. an extension of the moisture absorption work to a range of temperature should yield information on thermal vibrations which could be correlated with the thermal data. Likewise studies of dimensional changes accompanying the absorption/desorption of moisture at different stages of the curing process might be expected to lead to the development of a product with improved sealing characteristics.

Acknowledgement

We wish to express our gratitude to the Science and Engineering Research Council for a CASE award received by one of us (J.O'D.).

References

1. C. HARWOOD, B. YATES and D. V. BADAMI, *J. Mater. Sci.* **14** (1979) 1126.
2. S. SPEIL and J. P. LEINEWEBER, *Environmental Res.* **2** (1969) 166.
3. W. HOFMANN, "Vulcanization and Vulcanizing Agents" (Maclaren, London, 1967).
4. D. N. CASEY and B. YATES, *High Temp. High Press.* **6** (1974) 33.
5. D. A. DITMARS and T. B. DOUGLAS, *J. Res. Nat. Bur. Stand.* 75A (1971) 401.
6. V. Ya. LEONIDOV, *Geokhimiya* **4** (1967) 470.
7. T. A. HAHN, *J. Appl. Phys.* **41** (1970) 5096.
8. C. H. SHEN and G. S. SPRINGER, *J. Comp. Mater.* **10** (1976) 2.

Received 8 May
and accepted 1 June 1984